ACS APPLIED MATERIALS & INTERFACES

Research Article

www.acsami.org

Nonaqueous Atomic Layer Deposition of Aluminum Phosphate

Stefan Knohl,[†] Amit K. Roy,[†] Ralf Lungwitz,[‡] Stefan Spange,[‡] Thomas Mäder,[§] Daisy J. Nestler,[§] Bernhard Wielage,[§] Steffen Schulze,[⊥] Michael Hietschold,[⊥] Harm Wulff,[¶] Christiane A. Helm,[¶] Falko Seidel,[∥] Dietrich R. T. Zahn,[∥] and Werner A. Goedel*[,†]

[†]Physical Chemistry, Institute of Chemistry, Chemnitz University of Technology, Straße der Nationen 62, 09111 Chemnitz, Germany

[‡]Polymer Chemistry, Institute of Chemistry, Chemnitz University of Technology, Straße der Nationen 62, 09111 Chemnitz, Germany

[§]Institute of Material Science and Engineering, Institute of Mechanical Engineering, Chemnitz University of Technology, Erfenschlager Straße 73, 09125 Chemnitz, Germany

[⊥]Solid Surfaces Analysis Group, Institute of Physics, Chemnitz University of Technology, Reichenhainer Strasse 70, 09126 Chemnitz, Germany

[¶]Biophysics and Soft Matter, Institute of Physics, University Greifswald, Felix-Hausdorff Straße 6, 17487 Greifswald, Germany

[∥]Semiconductor Physics, Institute of Physics, Chemnitz University of Technology, Reichenhainer Straße 70, 09126 Chemnitz, Germany

Supporting Information

ABSTRACT: Aluminum phosphate was deposited onto bundles of carbon fibers and flat glassy carbon substrates using atomic layer deposition by exposing them to alternating pulses of trimethylaluminum and triethylphosphate vapors. Energy dispersive X-ray spectroscopy (EDXS) and solid state nuclear magnetic resonance (SS-NMR) spectra confirmed that the coating comprises aluminum phosphate (orthophosphate as well as other stoichiometries). Scanning electron microscopic (SEM) images revealed that the coatings are uniform and conformal. After coating, the fibers are still separated from each other like the uncoated fibers. Thermogravimetric analysis (TGA) indicates an improvement of oxidation resistance of the coated fibers compared to uncoated fibers.

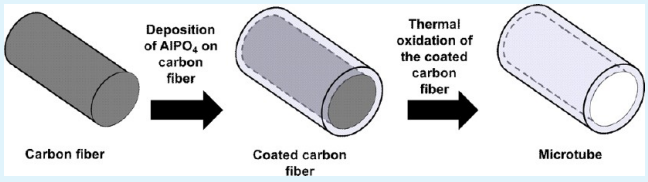

KEYWORDS: *coatings, ceramics, fibers, metal organic chemical vapor deposition, aluminum phosphate, atomic layer deposition*

INTRODUCTION

Embedding fibers into ceramic matrices can yield composites of increased toughness through a distributed damage mechanism.[1] The predominant reason for this effect is that cracks propagating through the matrices do not crack the fibers. Thus, the mechanical load that otherwise would give rise to a large stress in a small volume at the tip of the crack is distributed over a large number of fibers, therefore yielding a reduced stress that is spread out over a large volume. This mechanism, however, needs a weak bonding between the fiber and the matrix.[2] This weak bonding may be achieved by weakening the matrix in proximity of the fiber. Often, this is achieved by covering the fiber with a "weak coating" before embedding. Examples of "weak coatings" are graphitic carbon or boron nitride.[3] Both coatings, however, are prone to oxidation, especially in moist and oxidative environments. Furthermore, coatings often are applied to fibers to protect them from chemical reaction with the matrix or with the atmosphere (especially in the presence of cracks). Therefore, it is desirable to implement coatings that may give rise to the desired "weak" bonding, are oxidation resistant, and may further act as diffusion barriers to protect the fiber.

In previous publications, we used atomic layer deposition (ALD) to deposit oxidation resistant coatings such as alumina and titania onto carbon fibers.[4,5] The properties typical for ALD (deep infiltration, precise thickness control, and conformity) were achieved, and the coatings were efficient in protecting the fibers against oxidation. However, none of these coatings can be considered as "weak". Thus, the goal of the present contribution is to develop an atomic layer deposition process to deposit a weak and oxidation stable coating onto carbon fibers. Various phosphates ($LaPO_4$, $CePO_4$, $Ti_3(PO_4)_2$, $Ca_3(PO_4)_2$, $AlPO_4$) may fulfill these requirements and can act as a weak interface with improved oxidation resistance and low permeability for oxygen.[6−8] Thus, phosphate coatings may replace other coatings currently used in fiber reinforced ceramic composites. Out of the potential precursors for these materials, the precursors that may be used to deposit $AlPO_4$ are the most volatile and least expensive. In addition, aluminum orthophosphate ($AlPO_4$) is a covalently bonded, electrically neutral, and chemically inert material. Because of these properties, it has widespread applications in additional fields like catalysis or microelectronics.[9,10] Polycrystalline forms of $AlPO_4$ can be used for microelectronic packaging. One of the polymorphs of

Received: March 26, 2013
Accepted: June 11, 2013
Published: June 11, 2013

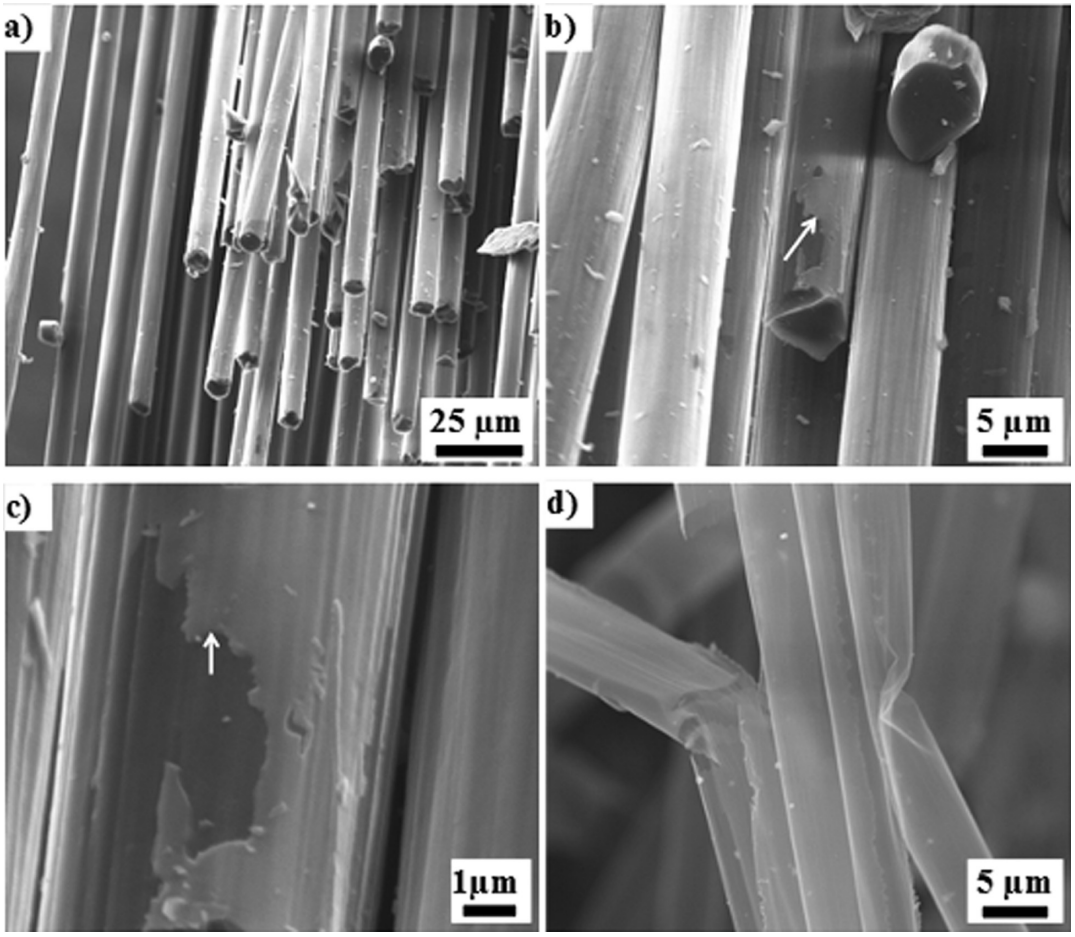

Figure 1. Scanning electron microscopic (SEM) images of (a–c) fibers coated at a temperature of 250 °C by 200 cycles of deposition and (d) $AlPO_4$ microtubes prepared via extended thermal oxidation of the coated fibers at 900 °C.

$AlPO_4$, berlinite, has piezoelectric properties.[11] Aluminum orthophosphates have interesting ion exchange and adsorption properties and may also be used in lithium ion batteries.[12,13]

Unlike h-BN and graphitic carbon, the aluminum phosphate is stable against water and oxygen up to 1400 °C[14,15] and thus can act as a diffusion barrier. Of special interest in our context is the fact that one of the polymorphs of the $AlPO_4$, tridymite, has a layered structure and thus can be considered a "weak" material.[16]

There are several reports about the synthesis of aluminum orthophosphates via sol–gel routes. In most of the sol–gel methods, phosphoric acid is used as a phosphate source. Sol–gel methods are limited, especially if uniform coatings onto individual filaments within fiber bundles are desired.[2] Additionally, in this method, aqueous sols of the precursors are used, which may be problematic for nonoxidic fibers (such as carbon and silicon carbide) because they might facilitate oxidative degradation. Thus, the sol–gel routes may not be an ideal deposition tool to coat reinforcing fibers, especially in the case of nonoxidic fibers.

Pure phosphoric acid is not an option as a precursor in vapor deposition processes because phosphoric acid has a very low vapor pressure at room temperature and heating leads to decomposition (mainly into P_2O_5 and water) instead of evaporation. Therefore, phosphate deposition has been limited by a lack of suitable precursors. There is a brilliant publication about thermal chemical vapor deposition (CVD) of aluminum phosphate onto glass by using single organometallic precursors, either $[Me_2AlO_2P(O^tBu)_2]_2$ or $[Al(O^iPr)_2O_2P(O^tBu)_2]_4$.[17] Unfortunately, these precursors are not yet commercially available but need to be synthesized prior to the deposition. Further processes for the deposition of phosphates like $LaPO_4$, $CePO_4$, $Ti_3(PO_4)_2$, $Ca_3(PO_4)_2$, and $AlPO_4$ were published recently[6,8,18]—including ALD processes[19,20]—and might be adopted for the coating of fibers. Here, we use an ALD process instead of a thermal single precursor CVD and expose bundles of carbon fibers to alternating pulses of vapors of the commercially available precursors, namely, trimethylaluminum ($AlMe_3$) and triethylphosphate ($OP(OEt)_3$). The goal is an atomic layer deposition process for a "weak" and oxidation stable coating onto carbon fibers.

■ RESULTS AND DISCUSSION

Aluminum phosphate was deposited onto bundles of carbon fibers and flat glassy carbon substrates. First, the fibers were exposed to alternating pulses of trimethylaluminum and triethylphosphate at reduced pressure and a temperature of 250 °C. Scanning electron microscopic (SEM) images of a part of the coated fiber bundle after this process are shown in Figure 1. Figure 1a,b reveal that the fibers within the bundle are still separated from each other, no bridges were formed, and the coatings reflect the original morphology of the fiber surface, and thus, no significant deviations from uniform deposition are visible. This latter fact is especially evident from Figure 1c

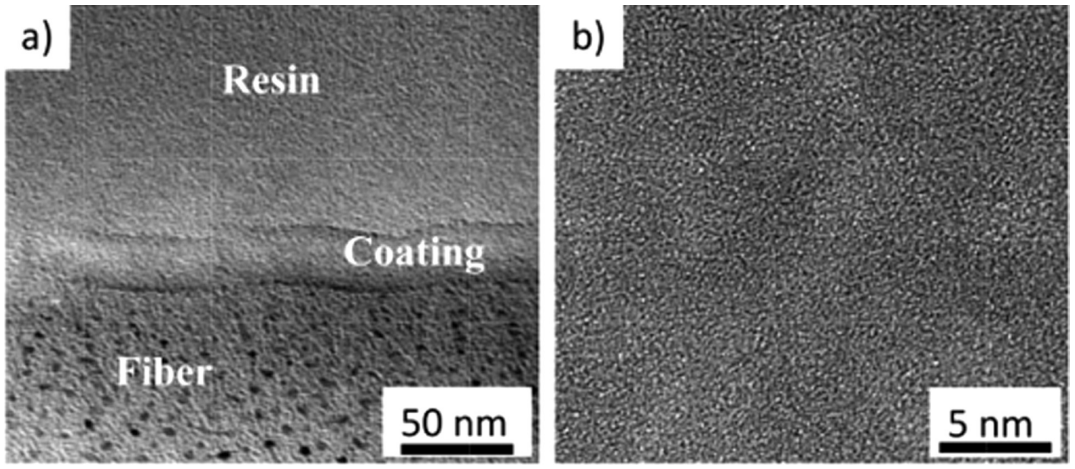

Figure 2. (a) Transmission electron microscopic (TEM) image of a cross-section through the surface of a single fiber coated via 250 cycles of deposition (sample was cut parallel to the fiber axis by a focused ion beam) and (b) image at higher magnification reveals an amorphous structure of the coating.

where the coating was partially removed and the underlying carbon fiber is visible. In these images, carbon fibers, which appear darker than the coatings, have the same surface structure as the coating. In our previous reports about alumina on carbon fibers, we observed delamination of coatings from the ends of cut fibers and the formation of clear straight steps.[5] In the case of the coatings shown here, we often observed no clear delamination, the border between coating and underlying fiber often being smeared out and forming an irregular line. Thus, it is likely that in the present case cohesion of the coating is weaker than its adhesion to the fiber. Thus, we might conclude that the coating may be considered as a "weak coating" at least in comparison to alumina. Transmission electron microscopy (TEM) images of a cross-section of a coating obtained after 250 cycles of deposition are shown in Figure 2. The interface between the fiber and the coating is sharp, and the coating is conformal (see Figure 2a). The high resolution image of this cross-section (Figure 2b) shows no indication of crystallites. Hence, the coating most probably is amorphous. The coating thickness obtained from the TEM image in Figure 2a is approximately 22 nm.

The thickness can as well be estimated from gravimetry (analyzing the mass of the residue left behind after complete oxidation in a thermogravimetric analysis). From these experiments, we obtain the thickness of the coatings as a function of total number of deposition cycles shown in Figure 3. The data points can be represented by a straight line with a slope of 0.082 nm/cycle ± 0.006 nm/cycle. This slope is in reasonable agreement with the deposition rate estimated from the TEM image in Figure 2a.

Elemental analysis of a fiber coated at a temperature of 250 °C by energy dispersive X-ray spectroscopy (EDXS; see Supporting Information) revealed a dominating carbon content as well as aluminum, oxygen, and phosphorus. The dominating amount of carbon was expected because of the carbon fiber; the presence of aluminum, oxygen, and phosphorus confirms the expected aluminum phosphate coating.

In addition to EDXS of the coated fibers, we removed the fiber by thermal oxidation in air at 500 °C and 900 °C over extended time spans and analyzed the composition of the residue which was left behind. As already observed in the case of alumina coating,[21] this residue has the shape of microtubes of the same diameter as the original fibers and thus is

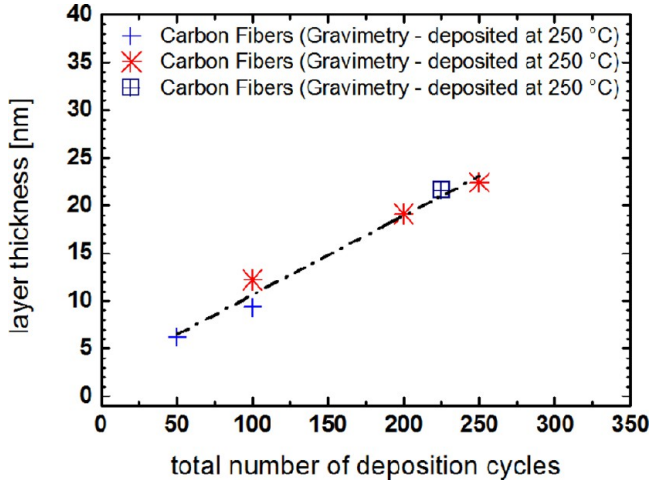

Figure 3. Coating thickness as a function of the number of cycles for coated carbon fibers. The coating thickness increases almost linearly with the number of cycles at an average deposition rate of 0.082 nm/cycle ± 0.006 nm/cycle.

predominantly composed of the coating (Figure 1d). In contrast to the alumina microtubes described earlier,[21] the microtubes observed here may be bent without breaking them (see Figure 1d). This behavior might further indicate the "weak" nature of the coating. This residue was characterized by elemental flash analysis, spectroscopic elemental analysis (inductive coupled plasma optical emission spectroscopy (ICP-OES) and wet chemical photometry), and solid state nuclear magnetic resonance (SSNMR). Elemental flash analysis (which is sensitive to C, H, and N) revealed a mass fraction of carbon, hydrogen, and nitrogen of 0.041, 0.016, and <0.0001. The molar ratio of phosphorus to aluminum in the coating was analyzed via ICP-OES. We observed molar ratios varying from sample to sample in a range between P/Al = 0.18 (Al/P = 5.5) and P/Al = 0.33 (Al/P = 3). These results were confirmed independently by wet chemical photometry. From the stoichiometry of aluminum orthophosphate, we expect a molar ratio of P/Al equal to 1. Hence, the amount of phosphorus is less than aluminum, and we are still away from the ideal stoichiometry. This excess of alumina compared to the ideal stoichiometry is similar to the compositions reported in

ref 19 in which trimethylphosphate and aluminum trichloride were used as precursors. The reason for this deviation is not clear to us. As discussed by the authors of ref 19, most probably the reaction of the phosphoric ester with the surface is slow or hindered.

^{27}Al and ^{31}P solid state nuclear magnetic resonance (SS-NMR) spectroscopy was used in order to investigate the molecular structure and the chemical composition of the residue left behind after oxidation in air at 500 °C and 900 °C, respectively. The ^{27}Al and ^{31}P NMR spectra of both samples are shown in Figure 4. In each ^{31}P NMR spectrum (Figure 4a), one

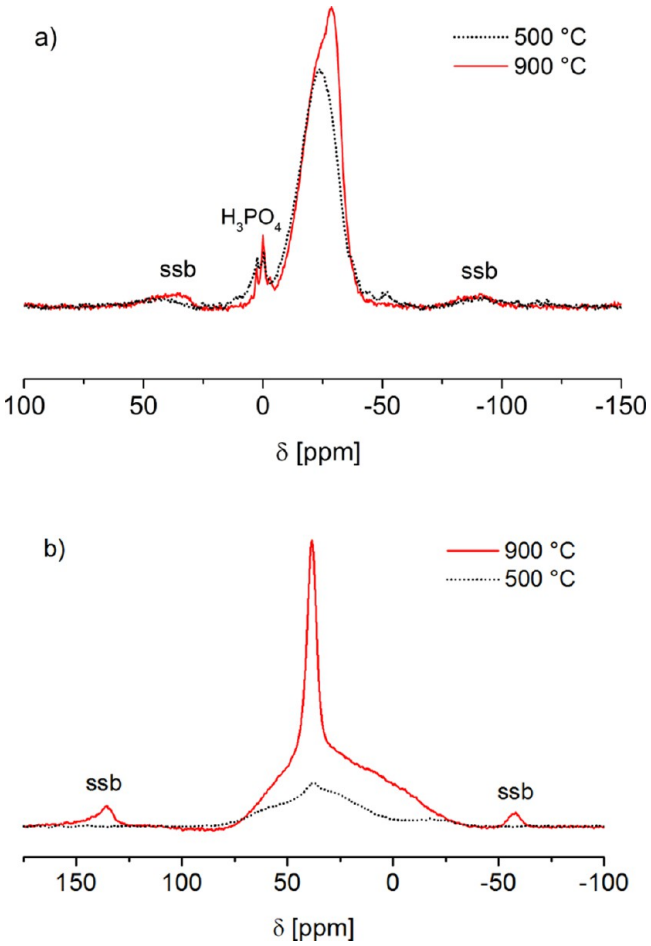

Figure 4. Solid state nuclear magnetic resonance (SS-NMR) spectra of the residue left behind after extended oxidative degradation of coated fibers in air at 500 °C (black dotted line) and at 900 °C (red line). (a) ^{31}P spectra and (b) ^{27}Al spectra. The bands labeled "ssb" are spinning side bands.

broad peak at −24 ppm (500 °C) and −29 ppm (900 °C), respectively, is observed. This peak is a result of three superimposed peaks, which can be assigned to phosphorus atoms with four oxygen atoms as nearest neighbors and with four (∼−30 ppm, Q_4^0), three (∼−21 ppm, Q_3^0), and two (∼−14 ppm, Q_2^0) aluminum atoms as next nearest neighbors.[22,23] The variation in the chemical shift of the maximum of the apparent peak with temperature used in the oxidative degradation of the fiber can be explained by varying amounts of the above mentioned phosphorus species. The ^{31}P NMR spectrum of the residue obtained via oxidation at 900 °C shows a peak maximum at −29 ppm close to the position of the Q_4^0 and a shoulder at lower field strength which can be assigned to Q_3^0 and Q_2^0. In comparison, the peak maximum in the ^{31}P NMR spectrum of the residue obtained via oxidation at 500 °C is shifted to −24 ppm indicating a lower amount of Q_4^0 species. In both ^{31}P NMR spectra, an additional peak at 0 ppm is observed which can be assigned to phosphoric acid (presumably formed due to reaction of phosphorus oxides with ambient moisture after the deposition or oxidation process). The ^{31}P NMR spectrum of the residue obtained via oxidation at 500 °C shows a small additional peak at −50 ppm corresponding to $Al(PO_3)_3$. This peak is missing in the spectrum of the residue obtained via oxidation at 900 °C.

Both ^{27}Al NMR spectra (Figure 4b) show a major peak at 38 ppm and shoulders at higher and lower field strength with varying intensity. The peak at 38 ppm can be assigned to ^{27}Al units in aluminum phosphate glass composed of alternating $Al(OP)_4$ and $P(OAl)_4$ tetrahedra. Its position is identical to the one of pure (crystalline) aluminum orthophosphate.[23]

In addition, there are shoulders that can be assigned to ^{27}Al species of varying number of oxygen atoms in their vicinity and varying number of phosphorus atoms in the second coordination sphere. In general, an increasing number of oxygen atoms as neighbors and an increasing number of phosphorus in the second coordination sphere shift the peak position to lower values.[22−25] Thus, the shoulder at about 60 ppm can be assigned to ^{27}Al atoms with four oxygen atoms as next neighbors but more aluminum than phosphorus atoms in the second coordination sphere. The shoulder at higher field strength is of a more complex nature, because there are various aluminum species that show peaks in the region between 30 ppmand −25 ppm. It may comprise ^{27}Al with five oxygen atoms as next neighbors and ^{27}Al atoms with six oxygen atoms as next neighbors with varying numbers of phosphorus in the second coordination sphere. The intensity of the peak at ∼38 ppm, which is characteristic for alternating $Al(OP)_4$ and $P(OAl)_4$ tetrahedra, is higher in the sample obtained at an oxidation temperature of 900 °C than in the sample obtained at 500 °C. In conclusion, ^{27}Al and ^{31}P solid state NMR spectroscopy evidence the presence of (disordered) aluminum orthophosphate with varying contents of Al−O−Al, P−O−P, and Al−O−P bridges. The relative content of Al−O−P bridges increases at higher annealing temperatures.

One of our goals was to improve the oxidation resistance of the carbon fibers. Thus, the oxidation resistance of coated and uncoated fibers was characterized by thermogravimetric analysis (TGA): 5 mm long coated fiber specimens were heated from 30 °C to 900 °C with a heating rate of 5 °C/min and subsequently held at 900 °C for 30 min in a flow of synthetic air. The results are shown in Figure 5; at the heating rate chosen, the oxidation onset temperature (3% weight loss) for the uncoated fibers is approximately at 630 °C and the fibers are completely burned at temperatures of approximately 825 °C. On the other hand, fibers coated with 33 nm and 135 nm thick layers of alumina start to oxidize at approximately 630 °C and 660 °C, respectively.[5] In the case of fibers coated with a 25 nm thick layer of aluminum phosphate, the oxidation starts at a temperature of approximately 700 °C and the fibers are not completely burned when the temperature of 900 °C is reached, but they need approximately 20 min additional time at that temperature to be completely oxidized. If heated for extended periods in air, fibers degrade even at lower temperatures; for example, a piece of 30 cm long fibers coated with 25 nm of aluminum phosphate need 4.5 h to be completely oxidized at

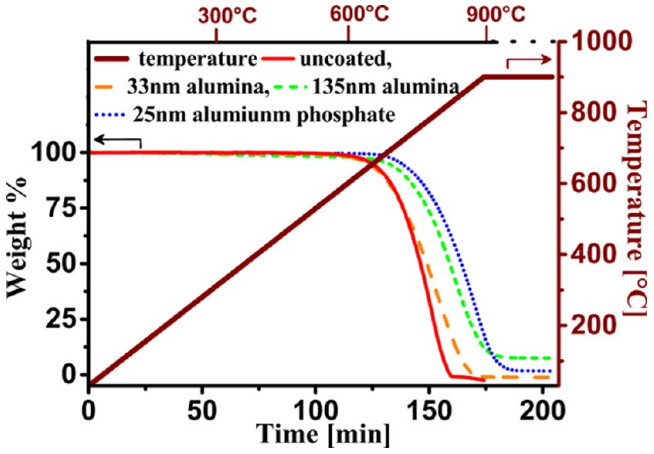

Figure 5. Thermogravimetric analysis of carbon fibers, uncoated (red continuous line) and coated with alumina (orange and green dashed line)[5] and aluminum phosphate (blue dotted line). The specimens were heated from 30 °C to 900 °C with a heating rate of 5 °C/min and subsequently held at 900 °C for 30 min in synthetic air.

900 °C and 137.5 h to become completely oxidized at 500 °C. Fibers coated with alumina of comparable thickness needed approximately a tenth of this time[21] to be completely oxidized by extended exposure to air at 500 °C. Thus, aluminum phosphate improves the oxidation resistance of the carbon fibers to some extent and seems to be even better than alumina coatings of a significantly higher thickness. The reason for the higher oxidation protection by aluminum phosphate compared to alumina is not completely elucidated yet. We note that in both cases oxidation proceeds uniformly over the whole length of the fiber and not from the cut ends on. Thus, it involves transport processes through the coating. Aluminum phosphate is reported to have a low oxygen permeability;[14,15] furthermore, the flexibility of the residual microtubes compared to alumina microtubes might indicate that the aluminum phosphate coating may have a lower tendency to form microcracks.

The thickness of a coating can be determined more accurately on a planar substrate than on a fiber. To show that the thickness of the coating is a linear function of the deposition cycles and in agreement with the rate expected for an ALD process, flat glassy carbon substrates were coated and the coating thickness was measured. Figure 6a shows a SEM image of the homogeneous uncoated surface. After 350 cycles of deposition, the sample surface image was still uniform with the exception of a few additional protuberances (Figure 6b).

Ellipsometry spectra were taken at 21 points regularly distributed over a sample area of 0.8 cm × 1.8 cm. The thickness of the coating derived from these measurements is shown in Figure 7. (For additional samples which confirm the results shown here, see the Supporting Information.) On the basis of the spectroscopic ellipsometry data, we calculated an average deposition rate of 0.136 nm/cycle ± 0.005 nm/cycle. These findings were confirmed further by X-ray reflectometry (Figure 8). Thus, as in the case of coated fibers (Figure 2) as well as in the case of flat substrates, the dependence of the thickness on the total number of deposition cycles may be represented by a straight line. The average deposition rates in both cases are in reasonable agreement with each other (on fibers: 0.082 nm/cycle ± 0.006 nm/cycle; on flat substrates: 0.136 nm/cycle ± 0.005 nm/cycle).

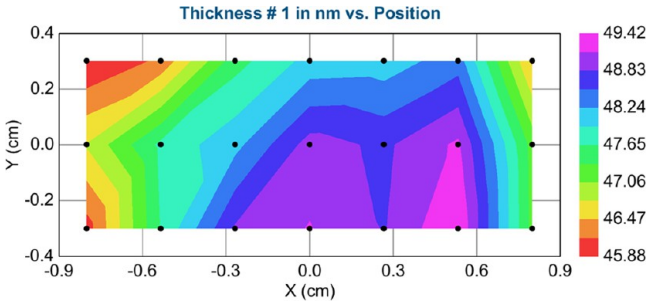

Figure 7. Thickness mapping via spectroscopic ellipsometry of a coating deposited onto a flat glassy carbon substrate via 350 cycles at a temperature of 250 °C, showing that the coating is uniform.

CONCLUSION

In conclusion, coatings comprising a significant amount of disordered aluminum phosphate ($AlPO_4$, as well as $Al(PO_3)_3$) were successfully deposited onto carbon fibers and flat glassy carbon substrates by atomic layer deposition. These layers were smooth, uniform, and conformal and provided protection against oxidation. The molar ratio P/Al of the coatings was

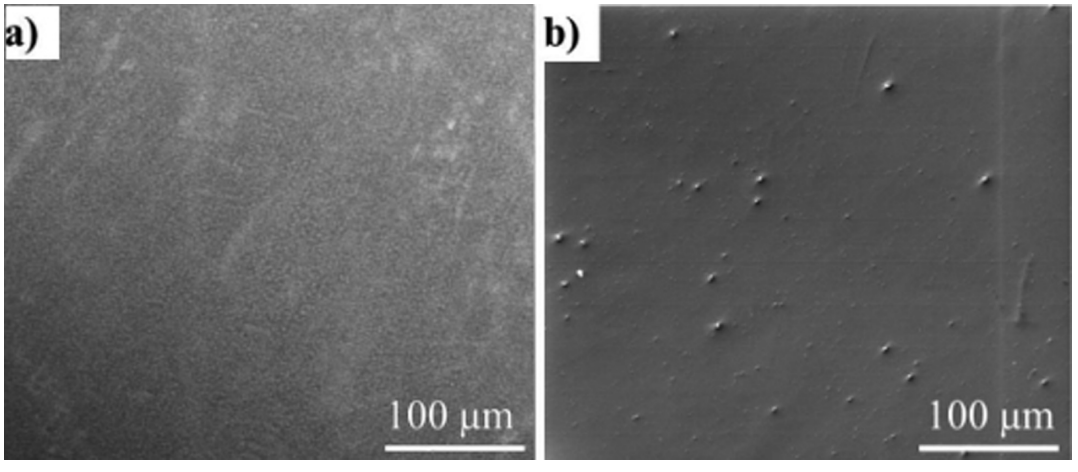

Figure 6. Scanning electron microscopic images of (a) an uncoated flat glassy carbon substrate and (b) aglassy carbon substrate coated at 250 °C by 350 deposition cycles.

dx.doi.org/10.1021/am401092z | ACS Appl. Mater. Interfaces 2013, 5, 6161−6167

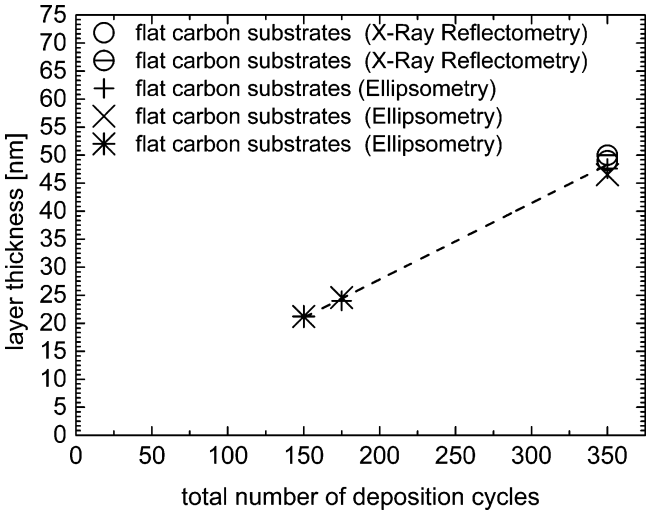

Figure 8. Thickness of layers deposited onto flat glassy carbon substrates as a function of the number of deposition cycle. The layer thickness increases almost linearly with the number of cycles at an average deposition rate of 0.136 nm/cycle ± 0.005 nm/cycle.

found to vary from deposition to deposition in the range of 0.18 to 0.33. Hence, further investigations will be needed if pure aluminum orthophosphate coatings are desired.

EXPERIMENTAL SECTION

Tenax HTA 5331 6K, PAN-based carbon fiber bundle (6000 fibers per bundle), was purchased from TOHO TENAX. As obtained, the fiber bundles bear a polymeric sizing. This sizing was removed by thermal treatment at 700 °C in N_2 atmosphere. Flat substrates of glassy carbon (1 cm × 2 cm) were purchased from HTW Hochtemperatur-Werkstoffe GmbH, Thierhaupten, Germany, and used as received. The reaction chamber and sample holder are identical to those described in ref 4. Briefly, the reactor is a 1 m long steel tube connected at one end to the supply vessels for the precursors via computer controlled valves and to the purge gas via mass flow controllers and at the other end to a rotary vane pump (PFEIFFER VACUUM, Duo 20, Mod. Nr.: PK D63 021) via another computer controlled valve. 3.6 m long segments of the fibers were mounted within the reactor onto a fiber holder in such a way that they were longitudinal oriented within the reaction tube and gently bent by 180° at the ends facing the precursor flow and the pump. Fibers are coated at a temperature of 250 °C using pulses of trimethylaluminum (98% from ABCR GmbH & Co KG, Karlsruhe) and of triethylphosphate (99% from ABCR GmbH & Co KG, Karlsruhe) in a home-built reactor. The supply vessel of trimethylaluminum was heated to 60 °C. The temperature of the triethylphosphate supply was maintained at 110 °C. Two streams of nitrogen were used as carriers for trimethylaluminum and triethylphosphate, respectively, as well as purge gas, their flow being controlled by two mass flow controllers each set to 20 standard cubic centimeters per minute (sccm). In the first half of the cycle, the fiber bundle was exposed to trimethylaluminum for 20 s followed by purging the reactor with nitrogen for 30 s. In the second half of the cycle, it was exposed to triethylphosphate for 20 s followed by purging the reactor with nitrogen for 30 s. In both exposures, the valve in front of the pump was closed; it was opened fully during the purge time.

Scanning electron microscopy (SEM) was recorded using a NanoNovaSEM (Philips), directly taking the specimens from the bundles after deposition. The same instrument was used to perform energy dispersive X-ray spectroscopy (EDXS). Samples for imaging with transmission electron microscopy (TEM) in Figure 2 were prepared using a focused ion beam (FIB, SEM NEON40EsB with EDXS and EBSD) and measured with a Philips CM 20 FEG. The details of this method were reported elsewhere.[26]

Thermogravimetry was performed using a TGA7 from PerkinElmer. Five mm long coated fiber specimens (weight varying between 1.0 mg and 1.4 mg) were heated from 30 to 900 °C with a heating rate of 5 °C/min and subsequently held for 30 min at 900 °C in 20 mL per min in synthetic air flow.

Fibers were removed after coating by thermal oxidation of 30 cm long segments exposed to air for extended time periods at 900 °C/4.5 h and at 500 °C/137.5 h. The residue left behind after thermal oxidation was investigated via electron microscopy and NMR-spectroscopy.

ICP-OES measurements for determination of the elements aluminum and phosphorus were performed by an external service provider (Berghof, Germany). Several samples were digested in aqua regia prior to measurement by the service provider; other samples were digested in our lab by hydrochloric acid and deionized water (3 mL of HCl, 36% by weight, Merck; 7.5 mL of deionized water) at a temperature of 130 °C in an autoclave with PTFE lining. There was no significant influence of the digestion method on the results obtained by ICP-OES.

Wet chemical analysis was performed by digestion in hydrochloric acid as described above. Separation of the aluminum ions from phosphate ions was achieved via ion exchange. This was followed by serial dilution in a buffer (acetic acid acetate, pH = 4.6) and quantitative spectrophotometrical analysis of the reaction products formed with Alizarin (aluminum) or ammonium heptamolybdate (phosphate).

Solid state NMR measurements were carried out at ambient temperature using a Bruker Avance 400 spectrometer and a double tuned 4 mm MAS (magic angle spinning) probe. At the field strength of 9.4 T, the resonance frequencies were 104.26 MHz for ^{27}Al and 161.97 MHz for ^{31}P. All spectra were recorded at a MAS rotation frequency of 12.5 kHz using zirconium oxide rotors. Typical acquisition parameters were pulse length 4.1 μs (90°) for ^{27}Al and 4 μs (40°) for ^{31}P and recycle delay 5 s (^{31}P) and 8 s (^{27}Al), respectively. The ^{27}Al and ^{31}P NMR chemical shifts were referenced to 1 M $Al(NO_3)_3$ aqueous solution (0 ppm) and 85% H_3PO_4 (0 ppm), respectively.

X-ray reflectometry on flat carbon substrates was performed using a θ–2θ diffractometer D 5000 (Siemens) with Cu Kα radiation (40 kV, 40 mA) equipped with a special sample stage for the reflectometry measurements. For data analysis, the software Leptos (Bruker AXS) was used.

Variable angle spectroscopic ellipsometry (VASE) was performed using a TSolar M2000 from J. A. Woollam, Inc. This setup measures in the photon energy range of 0.70 eV to 5.00 eV in steps of 0.02 eV. It enables one to map an area of 1 cm^2 range with a spot size of approximately 0.5 mm^2 on the sample surface. VASE measures the change of polarization state after reflection of light from a sample surface. The common terms presented in the literature[27] are ψ and Δ which are defined in eq 1.

$$\frac{\tilde{r}_p}{\tilde{r}_s} \equiv \tilde{\rho} = \tan\psi \cdot \exp(i\Delta) \tag{1}$$

The Fresnel coefficients for parallel and perpendicular polarized light are given by $\tilde{r}_p$ and $\tilde{r}_s$, respectively. The measured parameters ψ and Δ were modeled using the CompleteEASE evaluation software. The model assumes an $AlPO_4$ film is placed onto a semi-infinite glassy carbon substrate. An uncoated reference substrate was used to measure the glassy carbon dielectric function $\tilde{\varepsilon}_{glC}$ (for quasi semi-infinite samples, the dielectric function directly derives from $\tilde{\rho}$ [27]). This result compares well with data from the literature.[28] The thickness of the coating D_{AlPO4} was evaluated using an approach after Cauchy[27,29] which describes the dispersion of $n(\lambda)$ in a wavelength range with negligible κ as a polynomial in (λ^{-2}):

$$n(\lambda) = A + \frac{B}{\lambda^2} + \frac{C}{\lambda^4} \quad \text{for } \kappa = 0 \text{ and } A > B > C \tag{2}$$

The evaluation of these spectra was performed using eq 1 between 0.7 and 2.5 eV where $AlPO_4$ is known to be transparent.[30] The fitting

leads to the following Cauchy parameters: $A = 1.5^{+0.01}_{-0.05}$ μm^2 and $B = 0.02^{+0.003}_{-0.006}$ μm^2. The parameter C was assumed to be zero because $AlPO_4$ is a wide band gap material and high orders of dispersion become negligible in the investigated energy range. The thickness D_{AlPO4} was fitted by confining the Cauchy parameters A and B within the error bars for all three samples.

■ ASSOCIATED CONTENT

Supporting Information

Energy dispersive X-ray spectrum (EDXS) for a selected area 4.6 μm × 3.8 μm of a single fiber for 250 °C deposition temperatures and the corresponding elemental maps. Spectroscopic ellipsometry mapping results of the $AlPO_4$ thickness determined using the Cauchy model after eq 2. This material is available free of charge via the Internet at http://pubs.acs.org.

■ AUTHOR INFORMATION

Corresponding Author

*E-mail: werner.goedel@chemie.tu-chemnitz.de.

Notes

The authors declare no competing financial interest.

■ ACKNOWLEDGMENTS

We are grateful to Harry Rose, Micromanufacturing Technology, Chemnitz University of Technology, for designing the control software of the ALD reactor, Frank Diener and Frank Sternkopf from the workshop, Chemnitz University of Technology, for building components of the ALD reactor, and Maik Schlesinger and Lutz Mertens, Coordination Chemistry, Chemnitz University of Technology, whom we thank for measuring powder X-ray diffraction. We are thankful to Sabine Stöckel for the elemental analysis of the coatings with wet photometric analysis.

■ REFERENCES

(1) Naslain, R. R. *Composites, Part A: Appl. Sci.* **1998**, *29*, 1145−1155.
(2) Kerans, R. J.; Hay, R. S.; Parthasarathy, T. A.; Cinibulk, M. K. *J. Am. Ceram. Soc.* **2002**, *85*, 2599−2632.
(3) Naslain, R.; Dugne, O.; Guette, A.; Sevely, J.; Brosse, C. R.; Rocher, J. P.; Cotteret, J. *J. Am. Ceram. Soc.* **1991**, *74*, 2482−2488.
(4) Roy, A. K.; Baumann, W.; Konig, I.; Baumann, G.; Schulze, S.; Hietschold, M.; Mader, T.; Nestler, D. J.; Wielage, B.; Goedel, W. A. *Anal. Bioanal. Chem.* **2010**, *396*, 1913−1919.
(5) Roy, A. K.; Baumann, W.; Schulze, S.; Hietschold, M.; Mäder, T.; Nestler, D. J.; Wielage, B.; Goedel, W. A. *J. Am. Ceram. Soc.* **2011**, *94*, 3604−3604.
(6) Boakye, E.; Hay, R. S.; Petry, M. D. *J. Am. Ceram. Soc.* **1999**, *82*, 2321−2331.
(7) Bao, Y. H.; Nicholson, P. S. *J. Am. Ceram. Soc.* **2006**, *89*, 465−470.
(8) Mucalo, M. R.; Wielage, B.; Mucha, H. *J. Mater. Sci.* **2005**, *40*, 2671−2673.
(9) Parida, K.; Mishra, T. *J. Colloid Interface Sci.* **1996**, *179*, 233−240.
(10) Roy, D. M. *Science* **1987**, *235*, 651−658.
(11) Wang, H.; Xu, B.; Liu, X. L.; Han, J. R.; Shan, S. X.; Li, H. *J. Cryst. Growth* **1986**, *79*, 227−231.
(12) Kandori, K.; Ikeguchi, N.; Yasukawa, A.; Ishikawa, T. *J. Colloid Interface Sci.* **1996**, *182*, 425−430.
(13) Lee, H.; Kim, M. G.; Cho, J. *Electrochem. Commun.* **2007**, *9*, 149−154.
(14) Sambasivan, S.; Steiner, K. A. *High temperature amorphous composition based on aluminum phosphate*. US 6461415, 2002.
(15) Huang, J. F.; Yang, W. D.; Cao, L. Y. *J. Mater. Sci. Technol.* **2010**, *26*, 1021−1026.
(16) Kim, D. K.; Kriven, W. M. *J. Am. Ceram. Soc.* **2003**, *86*, 1962−1964.
(17) Lugmair, C. G.; Tilley, T. D.; Rheingold, A. L. *Chem. Mater.* **1999**, *11*, 1615−1620.
(18) Bao, Y. H.; Nicholson, P. S. *J. Eur. Ceram. Soc.* **2008**, *28*, 3041−3048.
(19) Hamalainen, J.; Holopainen, J.; Munnik, F.; Heikkila, M.; Ritala, M.; Leskela, M. *J. Phys. Chem. C* **2012**, *116*, 5920−5925.
(20) Wiedmann, M. K.; Jackson, D. H. K.; Pagan-Torres, Y. J.; Cho, E.; Dumesic, J. A.; Kuech, T. F. *J. Vac. Sci. Technol., A* **2012**, *30*, 01A134.
(21) Roy, A. K.; Knohl, S.; Goedel, W. A. *J. Mater. Sci.* **2011**, *46*, 4812−4819.
(22) Zhang, L.; Bogershausen, A.; Eckert, H. *J. Am. Ceram. Soc.* **2005**, *88*, 897−902.
(23) Zhang, L.; Eckert, H. *J. Mater. Chem.* **2004**, *14*, 1605−1615.
(24) Wegner, S.; van Wullen, L.; Tricot, G. *J. Non-Cryst. Solids* **2008**, *354*, 1703−1714.
(25) van Wullen, L.; Tricot, G.; Wegner, S. *Solid State Nucl. Magn.* **2007**, *32*, 44−52.
(26) Mucha, H.; Kato, T.; Arai, S.; Saka, H.; Kuroda, K.; Wielage, B. *J. Electron. Microsc.* **2005**, *54*, 43−49.
(27) Tomkins, H. G.; Irene, E. A. *Handbook of Ellipsometry*; William Andrew, Inc., Norwich; New York, 2005; p 12, 255, 282, 781.
(28) Deheer, W. A.; Bacsa, W. S.; Chatelain, A.; Gerfin, T.; Humphreybaker, R.; Forro, L.; Ugarte, D. *Science* **1995**, *268*, 845−847.
(29) Cauchy, A. L. *Mémoire sur la dispersion de la lumière*; J. G. Calve: Praque, 1836.
(30) Christie, D. M.; Troullier, N.; Chelikowsky, J. R. *Solid State Commun.* **1996**, *98*, 923−926.